Amino Acids (2010) 39:135–144
DOI 10.1007/s00726-009-0385-x

ORIGINAL ARTICLE

# LyeTx I, a potent antimicrobial peptide from the venom of the spider *Lycosa erythrognatha*

**D. M. Santos · R. M. Verly · D. Piló-Veloso · M. de Maria · M. A. R. de Carvalho · P. S. Cisalpino · B. M. Soares · C. G. Diniz · L. M. Farias · D. F. F. Moreira · F. Frézard · M. P. Bemquerer · A. M. C. Pimenta · M. E. de Lima**

Received: 19 September 2009 / Accepted: 29 October 2009 / Published online: 28 November 2009


**Abstract** LyeTx I, an antimicrobial peptide isolated from the venom of *Lycosa erythrognatha*, known as wolf spider, has been synthesised and its structural profile studied by using the CD and NMR techniques. LyeTx I has shown to be active against bacteria (*Escherichia coli* and *Staphylococcus aureus*) and fungi (*Candida krusei* and *Cryptococcus neoformans*) and able to alter the permeabilisation of L-α-phosphatidylcholine-liposomes (POPC) in a dose-dependent manner. In POPC containing cholesterol or ergosterol, permeabilisation has either decreased about five times or remained unchanged, respectively. These results, along with the observed low haemolytic activity, indicated that antimicrobial membranes, rather than vertebrate membranes seem to be the preferential targets. However, the complexity of biological membranes compared to liposomes must be taken in account. Besides, other membrane components, such as proteins and even specific lipids, cannot be discarded to be important to the preferential action of the LyeTx I to the tested microorganisms. The secondary structure of LyeTx I shows a small random-coil region at the N-terminus followed by an α-helix that reached the amidated C-terminus, which might favour the peptide-membrane interaction. The high activity against bacteria together with the moderate activity against fungi

A.M.C. Pimenta and M.E. de Lima have contributed equally to this work

**Electronic supplementary material** The online version of this article (doi:10.1007/s00726-009-0385-x) contains supplementary material, which is available to authorized users.

D. M. Santos · D. F. F. Moreira · A. M. C. Pimenta · M. E. de Lima (✉)
Lab. Venenos e Toxinas Animais,
Departamento de Bioquímica e Imunologia,
Instituto de Ciências Biológicas,
Universidade Federal de Minas Gerais,
Av. Antônio Carlos, 6627, 31270-901 Belo Horizonte,
Minas Gerais, Brazil
e-mail: melenalima@icb.ufmg.br; lima.mariaelena@gmail.com

R. M. Verly · D. Piló-Veloso
Departamento de Química, ICEX,
Universidade Federal de Minas Gerais,
Av. Antônio Carlos, 6627, 31270-901 Belo Horizonte,
Minas Gerais, Brazil

M. de Maria
Departamento de Zoologia,
Instituto de Ciências Biológicas,
Universidade Federal de Minas Gerais,
Av. Antônio Carlos, 6627, 31270-901 Belo Horizonte,
Minas Gerais, Brazil

M. A. R. de Carvalho · P. S. Cisalpino · B. M. Soares · L. M. Farias
Departamento de Microbiologia, Instituto de Ciências Biológicas, Universidade Federal de Minas Gerais,
Av. Antônio Carlos, 6627, 31270-901 Belo Horizonte,
Minas Gerais, Brazil

C. G. Diniz
Departamento de Parasitologia, Microbiologia e Imunologia,
ICB, Universidade Federal de Juiz de Fora,
36036-900 Juiz de Fora, Minas Gerais, Brazil

F. Frézard
Departamento de Fisiologia e Biofísica, Instituto de Ciências Biológicas, Universidade Federal de Minas Gerais,
Av. Antônio Carlos, 6627, 31270-901 Belo Horizonte,
Minas Gerais, Brazil

M. P. Bemquerer
Embrapa Recursos Genéticos e Biotecnologia, PqEB,
Av. W5 Norte (final), 70770-900 Brasília,
Distrito Federal, Brazil

and the low haemolytic activity have indicated LyeTx I as a good prototype for developing new antibiotic peptides.

**Keywords** *Lycosa erythrognatha* · Antimicrobial peptide · LyeTx I · Spider venom

## Introduction

Many antimicrobial peptides (AMPs) have been isolated from a wide range of eukaryotic and prokaryotic organisms (Kastin 2006) and may also occur as fragments of proteins, such as Buforin II (Park et al. 1994). AMPs show activity against a wide range of pathogens such as Gram-positive and Gram-negative bacteria, fungi and viruses (Hernández-Ledesma et al. 2008; Kastin 2006; Zasloff 2002; Mor and Nicolas 1994). These peptides usually show a high variability in their amino acid sequences, spanning from 7 to 55 amino acid residues, as well as a conservative net positive charge and an amphipathic secondary structure such as α-helix or β-sheet in lipid membrane milieu.

The action of eukaryotic AMPs is mediated by peptide-microbial cell membrane interactions resulting in membrane permeation and cell lysis, rather than by receptors (Zasloff 2002). The detailed mechanism of membrane disruption is not well understood, although physico-chemical data indicate that many peptides act as detergents while others act by promoting the formation of transient pores (Bechinger 2004; Verly et al. 2009). Nevertheless, there is no consensus up to now as to whether one or all of these models are correct. Furthermore, the AMP mechanism of action also depends upon a peptide secondary structure and aggregation tendency, as well as on the lipid composition of target membranes (Sanderson 2005).

Antimicrobial peptides have been found in arthropod venoms, mainly from spiders and scorpions (for reviewing see Kuhn-Nentwig 2009). The first description of antimicrobial activity in the venom of *Lycosa singoriensis* has been published in 1989 (Xu et al. 1989). Lycotoxins I and II, isolated from the wolf spider *L. carolinensis* venom were also reported (Yan and Adams 1998). These peptides display an amphipathic α-helix, typical of many very active AMPs, and show activity against Gram-negative bacteria (*Escherichia coli*) and yeast (*Candida glabrata*). AMPs from *L. singoriensis venom* (Xu et al. 1989; Budnik et al. 2004; Liu et al. 2009) with molecular masses in the range of 2,000–3,000 Da have also been isolated.

In this paper, we describe the primary and secondary structure together with the biological activity of LyeTx I, a new toxin from *L. erythrognatha* venom.

## Material and methods

### Spiders and venom collection and LyeTx I isolation

For the present study, spiders were collected in the regions of Belo Horizonte and Santa Bárbara (state of Minas Gerais, Brazil) and their venoms were collected via electrical stimulation of the fangs. Venoms were diluted in Milli-Q® water, immediately frozen in liquid nitrogen and then lyophilised.

### Chromatographic purification of LyeTx I

#### *Cation exchange chromatography*

The lyophilised venom was dissolved in Milli-Q water and loaded in a Cation exchange chromatography (CIEX) column (TSK gel CM-SW, 250 mm × 4.6 mm, Tosoh) equilibrated with solution A (10 mM sodium acetate buffer, pH 5). A linear salt gradient was made by increasing the solution B (10 mM sodium acetate buffer with 1 M NaCl, pH 5). 18–118 min, gradient of 0–85% solution B; 118–125 min, gradient of 85–100% solution B; 125–128 min 100% of solution B. The flow rate was set to 0.75 ml $min^{-1}$ with detection at 214 nm.

### Reversed-phase chromatography

The lyophilised fractions obtained from CIEX were dissolved in 0.1% aqueous trifluoroacetic acid (TFA) in Milli-Q water and loaded in a reversed-phase chromatography (RPC) column (Supelcosil™ C18, 25 cm × 4.6 mm) equilibrated with 0.1% aqueous TFA and eluted at a flow rate of 5 ml $min^{-1}$ with the following solutions: 0–5 min, a gradient of 0–45% acetonitrile in 0.1% TFA in water; 5–40 min, a gradient of 45–60% acetonitrile in 0.1% TFA in water; 40–45 min, gradient of 60–100% acetonitrile in 0.1% TFA in water; 45–55 min, 100% acetonitrile in 0.1% TFA; 55–60 min, 100–0% acetonitrile with 0.1% TFA in water. The flow rate was 1 ml $min^{-1}$ with detection at 214 nm.

### ESI-Q-TOF mass spectrometry analyses

ESI-Q-TOF mass spectrometry analyses were carried out by using a Q-TOF Micro (Micromass, Manchester, UK) equipped with an electrospray ionisation source operated in positive ion mode, as previously described (Pimenta et al. 2005). Briefly, capillary voltage was 2.5–3.0 kV and sample cone voltages were 40–60 V. Mass spectrometer calibrations were made by using sodium iodide with caesium iodide in 2,000 Da range. Samples were diluted in aqueous (Milli-Q water) acetonitrile solution (50% by volume)

containing 0.1% TFA and introduced by using a syringe pump with flow rates of 5–10 ml $min^{-1}$ in the electrospray source. Data were analysed by MassLynx® 4.0 software.

### MALDI-ToF/ToFMS analyses

MALDI-ToF/ToFMS analyses were performed using an ABI 4700 proteomics analyser with ToF/ToF optics (Applied Biosystems, USA), as previously described (Prates et al. 2004). Briefly, samples diluted in acetic acid (0.1%) were spotted onto a sample plate mixed with a saturated solution of α-cyano-4-hydroxycinnamic acid (CHCA) and allowed to dry at room temperature (dried-droplet method). The MS and the MS/MS spectra were acquired in the reflector mode with external calibration, using the calibration mixture Sequazyme standard kit (Applied Biosystems, USA). De novo peptide sequencing was performed by precursor ion fragmentation using $N_2$ as CID gas with collision cell pressure kept at $2.8 \times 10^{-6}$ Torr. Post-source decay spectra were obtained by increasing the laser energy and turning off the collision gas, as specified by the manufacturer.

### Edman degradation

The purified peptide (1–5 nmol) was sequenced by Edman degradation (PPSQ-21A protein sequencer, Shimadzu, Tokyo, Japan) coupled to reversed-phase separation of the PTH-amino acids on a WAKOSIL-PTH (4.6 mm × 250 mm) column (Wako, Osaka, Japan).

### Peptide synthesis and purification

The peptide was synthesised by stepwise solid-phase using the *N*-9-fluorenylmethyloxycarbonyl (Fmoc) strategy (Chan and White 2000) on a Rink amide resin (0.68 mmol $g^{-1}$). Side chain protecting groups were as follows: *t*-butyl for threonine, *t*-butyloxycarbonyl for lysine and tryptophan, (triphenyl)methyl for histidine, asparagine and glutamine. Couplings were performed with 1,3-diisopropylcarbodiimide/1-hydroxybenzotriazole in *N*,*N*-dimethylformamide (DMF) for 60–180 min. Deprotections (15 min, twice) were conducted by piperidine:DMF (1:4; v:v). Cleavage from the resin and final deprotection were performed with TFA/thioanisole/water/1,2-ethanedithiol/triisopropylsilane, 86.5/5.0/5.0/2.5/1.0, by volume) at room temperature during 90 min. After precipitating the product with cold diisopropyl ether, the crude peptide was extracted with aqueous acetonitrile at 50% by volume, freeze-dried and purified by RP-HPLC on a C18 semi-preparative column (Supelco, 5 μm, 250 mm × 10 mm) equilibrated with 0.1% aqueous TFA and eluted by a linear gradient of acetonitrile in 0.1% TFA (0–4 min, 0.1% TFA in water; 4–14 min, a gradient of 0–30% acetonitrile in 0.1% TFA in water; 14–82 min, gradient of 30–52% acetonitrile containing 0.1% TFA in water; 82–92 min, 52–100% acetonitrile containing 0.1% TFA in water; 92–102 min, 100% acetonitrile with 0.1% TFA. The flow was 3.0 ml $min^{-1}$ and detection at 214 nm.

### Antimicrobial tests

Reference bacteria strains, representative of Gram-positive (*Staphylococcus aureus* ATCC 33591) and Gram-negative (*Escherichia coli* ATCC 25922) bacteria, were cultured on brain heart infusion. The peptide susceptibility patterns were determined through the disk-diffusion method, based on the recommendations of the Clinical and Laboratory Standards Institute (CLSI 2007). Peptide stock solutions were applied on 0.5 mm diameter sterile filter discs and added to Muller-Hinton Agar plates (Difco Laboratories, USA). Bacterial strains were inoculated from a 0.5 McFarland bacterial suspensions to get a confluent growth. Inhibition growth zones were observed, measured and recorded.

The antifungal susceptibility tests were performed by the microdilution test according to CLSI (2002). The readouts were carried by determination of minimum inhibitory concentrations (MIC) defined as a reduction of 100% in growth after incubation at 35°C for 48 h (*Candida krusei*) and 72 h (*Cryptococcus neoformans*). Fluconazole was used as a control.

### Haemolytic assay

Rabbit erythrocytes, suspended in a phosphate-buffered saline (0.14 M NaCl; 2.7 mM KCl; 10 mM $Na_2HPO_4$, 1.8 mM $KH_2PO_4$, pH 7), were incubated with various peptide concentrations for 1 h at 37°C. Erythrocytes were then spun down and the released haemoglobin was measured spectrophotometrically at 405 nm. As a positive control for 100% of erythrocyte lysis, an aqueous Triton X-100 solution (1% by volume) was used instead of the peptide solution.

### Preparation of L-α-phosphatidylcholine-liposomes (POPC) and leakage of calcein assay

Small unilamellar vesicles (SUVs) were prepared as described previously (Frezard et al. 1994), through ultrasonication of multilamellar vesicles in the presence of 75 mM calcein at pH 7.2 and used within 48 h after preparation. Non-encapsulated calcein was removed from the calcein-containing liposomes through a Sephadex G-50 column equilibrated with 0.02 HEPES buffer containing 0.15 M NaCl, pH 7.2.

The peptide membrane-permeabilising activity was determined at 37°C by calcein leakage from SUVs that was monitored in HEPES buffer by fluorescence measurement (Cary Eclipse spectrofluorimetry, Varian, Palo Alto, USA) with excitation wavelength at 490 nm and emission wavelength at 515 nm. The maximum fluorescence intensity (100% leakage) was determined by adding 10 µl of an aqueous Triton X-100 solution (1% by volume) to the liposome sample (2.5 ml).

### Circular dichroism spectroscopy

Secondary structure preferences of LyeTx I were investigated at 298 K in the following milieu: aqueous media (100 µM phosphate buffer solution, pH 7.0 and 100 µM Tris–HCl buffer solution, pH 8.0), water/2,2,2-trifluoroethanol (TFE) mixtures, dodecylphosphocholine (DPC) micelles, 1-palmitoyl-2-oleoyl-*sn*-glycero-3-phosphocholine (POPC) and POPC/POPG (1-palmitoyl-2-oleoyl-*sn*-glycero-3-phosphoglycerol), at 3:1(w:w) SUVs. The equipment used was a Jasco-715 spectropolarimeter (Jasco, Tokyo, Japan) with a 1.0-mm rectangular quartz cuvette (Uvonic Instruments, Plainview, USA). Spectra were recorded from 260 to 190 nm using a 1.0-nm spectral bandwidth, 0.1 nm step resolution, 100 nm $min^{-1}$ scan rate and 4 s response time.

The peptide concentration, as determined from the tryptophan molar absorptivity ($\varepsilon = 5{,}550\ M^{-1}\ cm^{-1}$ at 280 nm), was at 10 µM in all CD studies. The obtained spectra were analysed using the CDPro software.

### NMR

The sample was prepared by dissolving the peptide at 2 mM in a solution of 400 mM $DPC_{d38}$, 5% (by volume) $D_2O$ and 10 $\mu$M 2,2-dimethyl-2-silapentane sulfonate and pH was adjusted to 7.0 with 20 mM phosphate buffer.

The NMR experiments were conducted at 20°C on a Bruker Avance DRX spectrometer [Centro Nacional de Ressonância Magnética Nuclear Jiri Jonas (CNRMN), Rio de Janeiro, Brazil] operating at 600,043 MHz for the $^1H$ frequency and using a triple-resonance ($^1H/^{13}C/^{15}N$) gradient probe (5 mm diameter)].

The Total Correlation Spectroscopy (TOCSY) spectra were acquired by using the MLEV-17 pulse sequence. The spectral width was determined as 6,900 Hz, and the 512 $t_1$ increments were collected with eight transients of 4,096 points. NOESY spectra were acquired using mixing times of 80, 100, 120, 140 and 160 ms. For this experiment, the spectral width was 6,900 Hz and the 512 $t_1$ increments were collected with 16 transients of 4,096 points for each F1. $^1H–^{13}C$ HSQC spectra were acquired with F1 and F2 spectral widths of 27,160 and 8,993 Hz respectively. 400 $t_1$ increments were collected with 56 transients of 1,024 points. The experiment was carried out in an edited mode in such a way that CH and $CH_3$ correlations could show a positive phase and $CH_2$ correlations, a negative phase. $^1H–^{15}N$ HSQC spectra were acquired with F1 and F2 spectral widths of 27,160 and 8,993 Hz, respectively. Eighty $t_1$ increments were collected (with 400 transients of 1,024 points), for each free induction decay. The NMR spectra were analysed using NMRVIEW, version 5.0.3.

### NOE data and structure calculations

The NMR spectra were analysed by using NMRVIEW, version 5.0.3. NOE intensities obtained at 120 ms mixing times were converted into semi-quantitative distance restraints using the calibration by Hyberts et al. (1992). The upper limits of the distance restraints thus obtained were 2.8, 3.4 and 5.0 Å for strong, medium and weak NOEs, respectively. Structure calculations were performed using the Xplor-NIH software, version 2.17.0. Starting with the extended structure, 200 structures were generated using a simulated annealing protocol. This was followed by 18,000 steps of simulated annealing at 1,000 K and a subsequent decrease in temperature in 9,000 steps in the first slow-cool annealing stage. The display, analysis and manipulation of the three-dimensional structures were performed with the programme MOLMOL. The stereochemical quality of the lowest energy structures was analysed by using the PROCHECK-NMR software (Laskowski et al. 1996).

## Results and discussion

The crude venom of the spider *L. erythrognatha* was fractionated by CIEX in HPLC and 16 fractions were manually collected and vacuum-dried, as shown in Fig. 1a. The main fraction (F12) was resuspended in distilled water and purified by RPC and six major subfractions were pooled (Fig. 1b). Subfraction 12.4 was analysed by mass spectrometry and a pure peptide with *m/z* 2831.1 was detected and named LyeTx I.

The primary structure of LyeTx I was determined up to the 19th amino acid residue by automated Edman degradation. Its molecular mass estimated from this partial sequence indicated that five to seven amino acid residues were still lacking. The sequence was completed by both ESI-Q-TOF and MALDI-TOF-TOF mass spectrometry analyses. The LyeTx I complete amino acid sequence was identified as

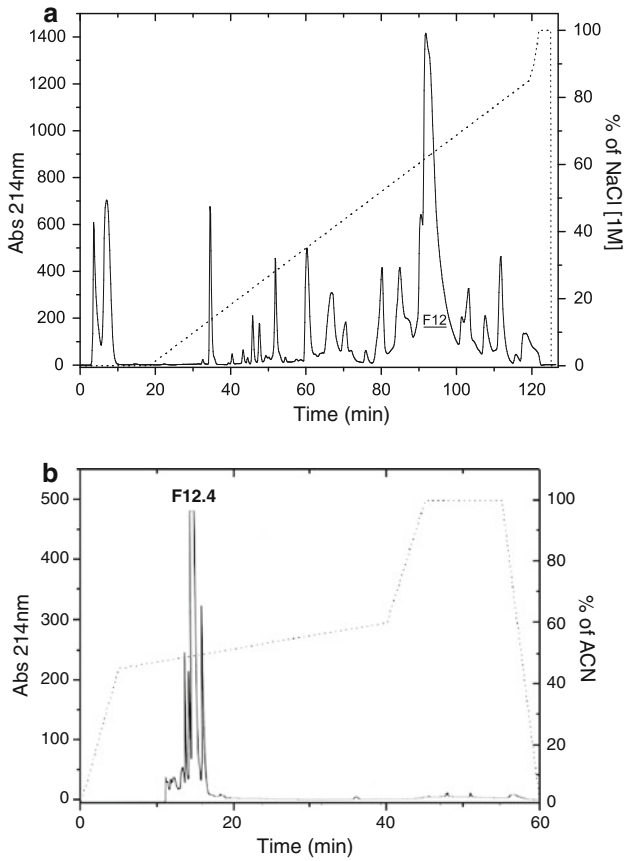


**Fig. 1** Purification of LyeTx I from spider venom by HPLC. **a** The supernatant of the centrifuged crude venom was applied to cation exchange HPLC (TSK gel CM-SW column, 4.6 mm × 250 mm, Tosoh), with a linear NaCl gradient up to 1 M. A linear salt gradient was made by increasing the solution B (10 mM sodium acetate buffer with 1 M NaCl, pH 5) 18–118 min, gradient of 0–85% solution B; 118–125 min, gradient of 85–100% solution B; 125–128 min 100% of solution B. The flow rate was 0.75 ml $min^{-1}$ and detection was at 214 nm. **b** The fraction F12 was re-purified by reversed-phase HPLC in a C18 Supercosil column (4.6 mm × 250 mm, Supelco) equilibrated with 0.1% aqueous TFA followed by a linear gradient of acetonitrile in 0.1% TFA. The elution was at a flow rate of 5 ml $min^{-1}$ with the following solutions: 0–5 min, a gradient of 0–45% acetonitrile in 0.1% TFA in water; 5–40 min, a gradient of 45–60% acetonitrile in 0.1% TFA in water; 40–45 min, gradient of 60–100% acetonitrile in 0.1% TFA in water; 45–55 min, 100% acetonitrile containing 0.1% TFA; 55–60 min, 100–0% acetonitrile with 0.1% TFA in water. The flow was 0.75 ml $min^{-1}$ and detection was at 214 nm

H-IWLTALKFLGKNLGKHLAKQQLAKL-$NH_2$ and, as compared to those of other AMPs, is highly similar (84%) to the Lycotoxin I (Yan and Adams 1998) (Table 1).

In order to study the antimicrobial activity and further explore its biological properties, LyeTx I was synthesised, using the Fmoc solid-phase strategy, and purified by reversed-phase HPLC (Fig. 2). Synthetic product identity was confirmed by ESI-Q-TOF MS observed ($M + H^+$) 2831.9; calculated ($M + H^+$) 2831.7.

**Table 1** Amino acid sequences of antimicrobial toxins

| | |
|---|---|
| LyeTx I | --IWLTALKFLGKNLGKHLAKQQLAKL---------- |
| Lycotoxin 1 | --IWLTALKFLGKHAAKHLAKQQLSKL---------- |
| Lycocitin | KIKWFKTMKSLAKFLAKEQMKKHLGE---------- |
| Lycotoxin 2 | KIKWFKTMKSIAKFIAKEQMKKHLGGE---------- |
| Dermaseptin 4 | -ALWMTLLKKVLKAAAKALNAVLVGANA---------- |
| Pleurocidin | --GWGSFFKKAA-HVGKHVGKAALTHY---------- |
| Moricin | AKIPIKAIKTVGKAVGKGLRAINIASTANDVFNFLKPKKRKA |
| Magainin 2 | ---GIGKFLHSAKKFGKAFVGEIMNS---------- |
| Cecropin E | RWKIFKKIEKVGQNIRDGIVKAGPAVAVVGQAATI------- |

Sequence alignment of LyeTx I against other amphipathic antimicrobial peptides. These sequences were aligned with Clustal W, using a PAM 250 matrix. Sequences are from the following references: Lycotoxin 1 and 2 (Yan and Adams 1998), Lycocitin (Budnik et al. 2004), Dermaseptin 4 (Mor and Nicolas 1994), Pleurocidin (Syvitski et al. 2005), Moricin (Hemmi et al. 2002), Magainin 2 (Zasloff 1987), Cecropin E (Boman and Hultmark 1987)

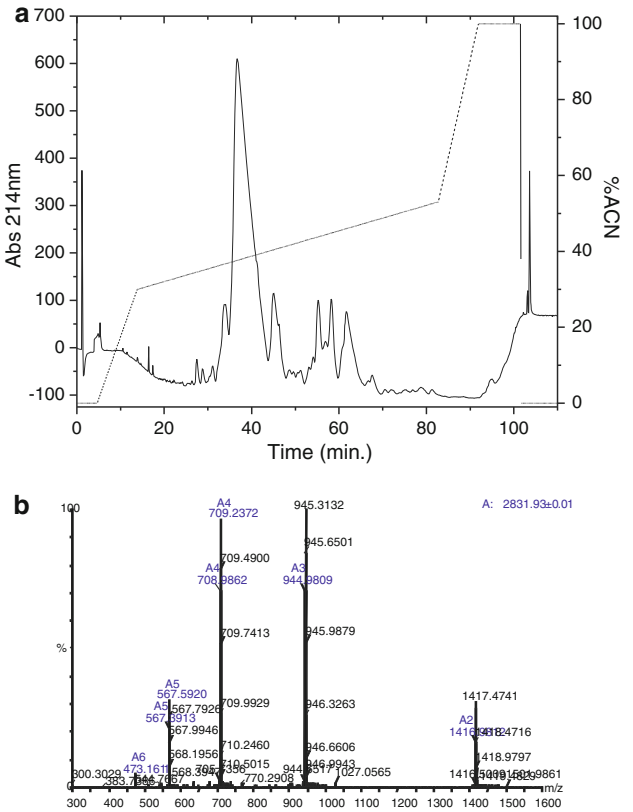


**Fig. 2** Purification of synthetic LyeTx I by HPLC. **a** Reversed-phase profile of the synthetic crude product. Supelcosil column (10 mm × 250 mm C18 Supelco) equilibrated with 0.1% aqueous TFA and eluted by a linear gradient of acetonitrile in 0.1% TFA. The flow was 3.0 ml $min^{-1}$ and detection was at 214 nm. **b** The fraction F12.4 was analysed by ESI mass spectrometry. A molecular mass was measured at 2831.93 Da, obtained by deconvolution of the MS-spectra

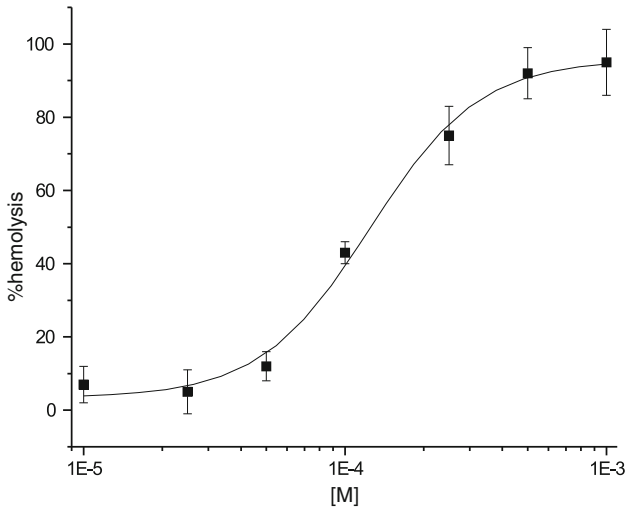


**Fig. 3** Hemolytic activity of LyeTx I. Rabbit erythrocytes suspended in PBS were incubated with increasing concentrations of synthetic LyeTx I for 1 h. The haemoglobin released in presence of Triton X-100 (1% by volume) was taken as 100% of cell lysis. Haemoglobin released was measured at 405 nm. $ED_{50} = 1.3 \times 10^{-4}$ M

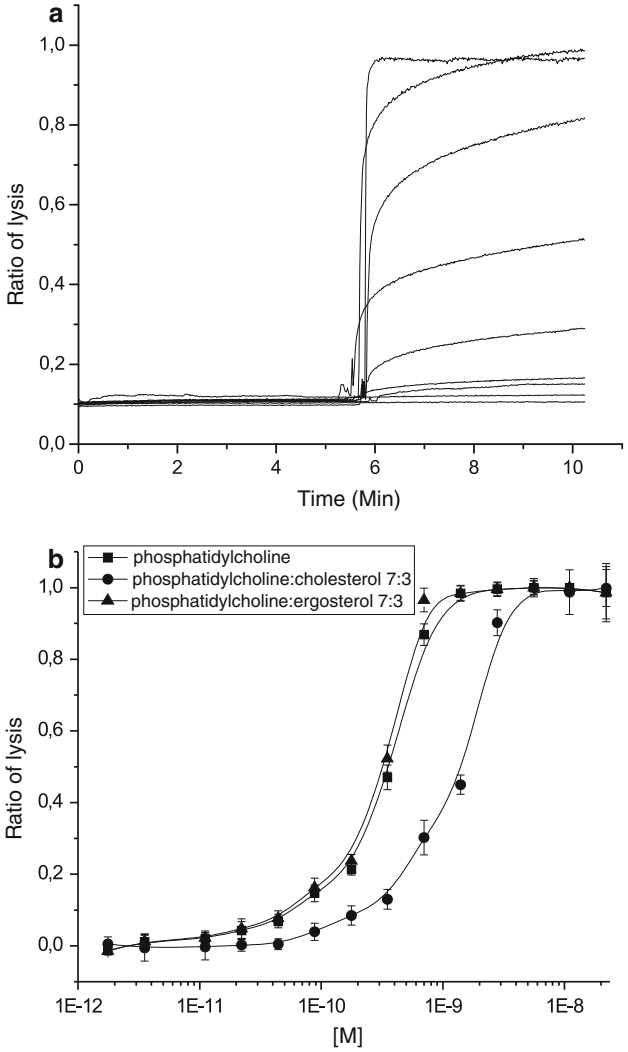


**Fig. 4** Leakage induced by LyeTx I of the fluorescent probe calcein from liposomes. **a** Kinetics of leakage of calcein from liposomes containing. L-α-phosphatidylcholine. LyeTx I at increasing concentrations (0.05, 0.1, 0.2, 0.4, 0.8, 1.6, 3.2, 6.4 and 12.8 μg $ml^{-1}$) was applied to the liposome suspension 6 min after incubation at 37°C. **b** Curves of concentration-dependence of calcein permeabilisation by LyeTx I in L-α-phosphatidylcholine liposomes, with or without addition of cholesterol or ergosterol at 7:3 molar ratio. Fluorescence emission was measured 2 min after incubation with the toxin. $ED_{50}$ for phosphatidylcholine liposomes was calculated at $2.7 \times 10^{-10}$ M, for phosphatidylcholine/cholesterol (7:3, molar ratio) liposomes at $8.2 \times 10^{-10}$ M and for phosphatidylcholine/ergosterol (7:3, molar ratio) lipids at $2.5 \times 10^{-10}$ M

## Antimicrobial and haemolytic assays of the synthetic peptide

The synthetic LyeTx I showed antimicrobial activities, although a comparison between the MIC values reported here and the results obtained by other authors with related peptides is rather difficult as different assay conditions and other strains of microorganisms are commonly employed. LyeTx I was active against the Gram-positive bacteria *S. aureus* (3.79 μM), the Gram-negative *E. coli* (7.81 μM) and against the yeasts *Candida krusei* (26.30 μM) and *Cryptococcus neoformans* (13.20 μM). Its antifungal activity is thus lower than its antibacterial activity when these organisms are taken into account. These data are similar to those reported for the Lycotoxins isolated from *L. carolinensis* and also for other AMPs (Yan and Adams 1998; Giacometti et al. 1999).

LyeTx I presented haemolytic activity (Fig. 3) in higher concentrations ($ED^{50} = 1.3 \times 10^{-4}$ M), when compared to values from antibacterial assays (i.e. in the micromolar range). The high activity of LyeTx I against bacteria, together with its moderate activity against yeasts and low haemolytic activity have set LyeTx I as a good candidate prototype for the development of new antibiotic peptides, especially for treating skin and mucosa bacterial infections. Chen et al. (2005) proposed that an increment in both positive charge and amphipathicity of peptide is important for bacterial lysis, while an increased hydrophobicity is correlated with erythrocyte lysis. Martins et al. (2006), working on peptides derived from Trialysin, a pore-forming protein found in the salive of *Triatoma infestans*, the insect vector of Chagas disease—proposed that the diversified lytic activity of some peptides against selected targets may be associated with the presence of specific structural details, while amphipathicity is essential for the lytic activity. Additionally, these authors have suggested that selectivity of active peptides for specific organisms appears to be associated with the structural features of their N-and C-termini (Martins et al. 2006). These structural

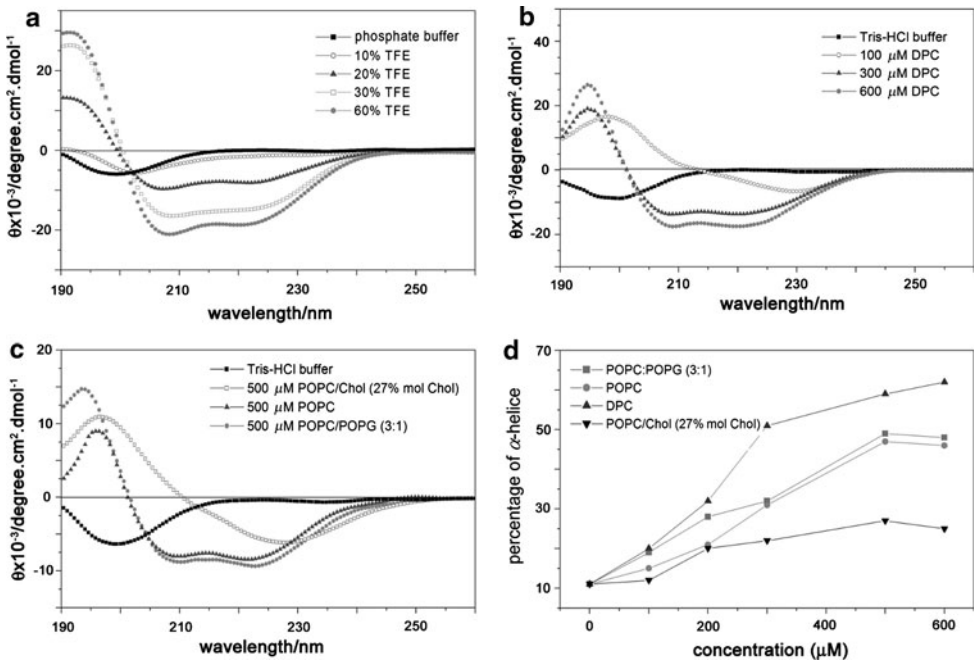


**Fig. 5** CD spectra of LyeTx I at 10 μM **a** in phosphate buffer, pH 7.0, containing no TFE (*dark filled square*), 10% (by volume) TFE (*open circle*), 20% TFE (*dark filled triangle*), 30% TFE (*open square*) and 60% TFE (*dark filled circle*); **b** in Tris–HCl buffer, pH 8.0, containing no DPC (*dark filled square*), 100 μM DPC (*open square*), 300 μM DPC (*dark filled triangle*) and 600 μM DPC; **c** in 500 μM POPC/Chol (27% mol cholesterol) SUVs (*open square*), 500 μM POPC SUVs (*dark filled triangle*) and 500 μM POPC:POPG (3:1, w: w) SUVs (*dark filled circle*). **d** Helical contents obtained from CD spectroscopy as a concentration function of the following media: DPC (*dark filled triangle*), POPC SUVs (*dark filled circle*), POPC-Chol (27% mol cholesterol) SUVs (*dark filled inverted triangle*) and POPC:POPG (3:1, w:w) SUVs (*dark filled square*)

features should be explored in the case of LyeTx I, in searching for analogues with higher specificity toward microorganisms of medical interest.

## LyeTx I induced permeabilisation of liposomes

Upon addition of LyeTx I (0.2 μg $ml^{-1}$) to L-α-phosphatidylcholine liposomes (POPC), the entrapped self-quenched calcein was immediately released, as it became evident by the increase of fluorescence intensity (Fig. 4a). The increments of fluorescence 2 min after adding the peptide are shown in Fig. 4b. The kinetics of calcein release was dose-dependent and that indicates a cooperative behaviour (Takeuchi et al. 2004).

The presence of cholesterol in POPC resulted in a less favourable insertion of AMPs into lipidic membranes, mainly by reducing the membrane fluidity (Matsuzaki et al. 1995; Verly et al. 2009). We observed that liposomes containing L-α-phosphatidylcholine:cholesterol (7:3 molar ratio) were approximately five times more resistant to the action of LyeTx I (Fig. 4b), when compared to those constituted only by L-α-phosphatidylcholine or of L-α-phosphatidylcholine:ergosterol (7:3 molar ratio).

## Circular dichroism spectroscopy

As shown in Fig. 5a, b, whereas the peptide exhibited predominantly random coil conformations in buffer solution at pH 7.0 or 8.0, characteristic curves of α-helix formation were obtained upon addition of 20% TFE (Fig. 5a) or up to 100 μM DPC micelles (Fig. 5b). This could be verified by the increase in CD amplitudes of the characteristic α-helix signals, with minima at 208 and 222 nm and a maximum at 192 nm. Adding 500 μM of POPC or POPC:POPG (3:1, w:w) SUVs to aqueous solutions (Tris–HCl buffer) of LyeTx I also caused a significant increase in the helical conformation (Fig. 5c). However, it should be noted that the degree of the helix formation decreased in the presence of 500 μM POPC containing 27% of cholesterol (SUVs POPC/Chol), indicating less structuration of the peptide.

The helix content as a function of lipid concentration is shown in Fig. 5d for LyeTx I. It can be observed that at about 500 μM lipids, LyeTx I have reached the full helical content in DPC, POPC and POPC/POPG, while the saturation was verified to be reached with a small helical content at 200 μM for POPC/Chol. Thus, it could be

concluded that the presence of cholesterol decreases the peptide–lipid interaction.

## NMR

The structure of LyeTx I was investigated by NMR spectroscopy in DPC, since CD studies indicate an elevated α-helical content of the peptide in these micelles (Fig. 5). Furthermore, the use of micelles is a better choice than TFE for membrane interface simulation. Sequence-specific chemical shift assignments were performed for LyeTx I from the correlations observed in TOCSY and NOESY spectra using standard procedures. The analysis of $^{1}H$–$^{15}N$ and $^{1}H$–$^{13}C$ HSQC spectra allowed the unequivocal assignment of all cross-peaks. A table showing $^{1}H$, $^{13}C$ and $^{15}N$ chemical shifts is given on supplementary material (SM-1). The fingerprint region of the TOCSY spectrum is presented in Fig. 6a, while the correlation between the amidic protons is shown in Fig. 6b. Other regions of spectra are given on supplementary material: tocsy-supplementary (SM-2), noesy-supplementary (SM-3), hsqc-$^{1}H^{15}N$-supplementary (SM-4), hsqc-$^{1}H^{13}C$-supplementary (SM-5). The high number of correlations between the amidic protons observed in the NOESY spectrum was consistent with a significant structural stability of the peptide in the micellar environment. Through-space and through-bond correlations between different residues were observed from the N-terminus up to the C-terminus (Fig. 7). Medium range NOE cross peaks involving the amidic protons were observed from the second residue up to the C-terminus, indicating a great ordering degree of the peptide structure. However, the NOESY spectrum exhibits more correlations between protons close to the amidated C-terminus than close to the unmodified N-terminus. This behaviour was already observed for other C-terminal amidated AMP peptides (Verly et al. 2009) and, moreover, those peptides often exhibited a higher antimicrobial activity than their non-amidated counterparts (Sforça et al. 2004). A total of 370 NOEs was observed posing distance restraints for estimating the twenty lowest energy structures for the LyeTx I molecule in the presence of DPC micelles (Fig. 8a). These structures were conformed as a slightly bent α-helix. Some observed inter-residue correlations involving Ile-1, Trp-2 and Leu-3 indicated that the N-terminus exhibited some structural order, albeit to a lesser extent than that of the C-terminus, as may be seen in Fig. 8a. Two correlations of the sort $d_{N,N}(i,\ i+2)$ observed - involving the Phe-8 and Gly-10, and Asn-12 and Gly-14 residues—are experimental evidences of the bend in the structures.

Therefore, the LyeTx I NMR structure shows similarity to that observed for the amphibian peptide DD K (Verly et al. 2009): a small random-coil region in the N-terminus

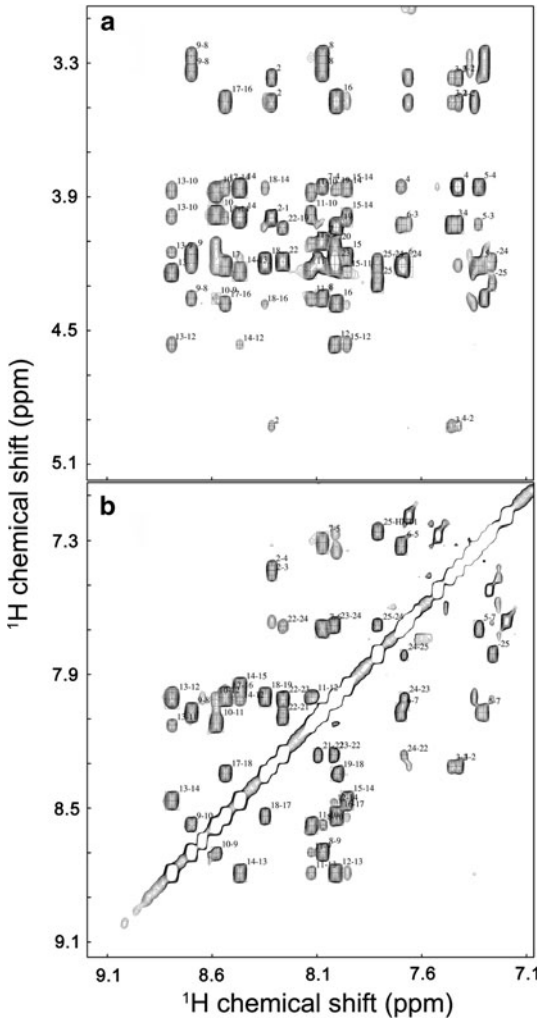


**Fig. 6** **a** NH–Hα region of the TOCSY spectrum of LyeTx I (at 2 mM) in 400 mM $DPC_{d38}$ micellar solution in $H_2O$:$D_2O$ (95:5, v:v). **b** NH–HN and H–H aromatic side chain region of the NOESY spectrum of LyeTx I (2 mM) in 400 mM $DPC_{d38}$ micellar solution in $H_2O$:$D_2O$ (95:5, v:v)

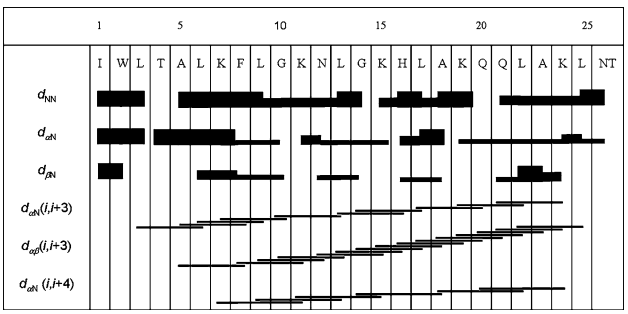


**Fig. 7** NOE connectivity diagram: Sequential NH($i$)–NH($i + 1$), Hα($i$)–NH($i + 1$), Hβ($i$)–NH($i + 1$) and medium range NH($i$)–NH($i + 2$), Hα($i$)–NH($i + n$), Hα($i$)–Hβ($i + n$)

followed by a helical segment that (for LyeTx I) is extended from Leu-6 up to the C-terminus. Nevertheless, LyeTx I structure shows a less amphipathic profile in the

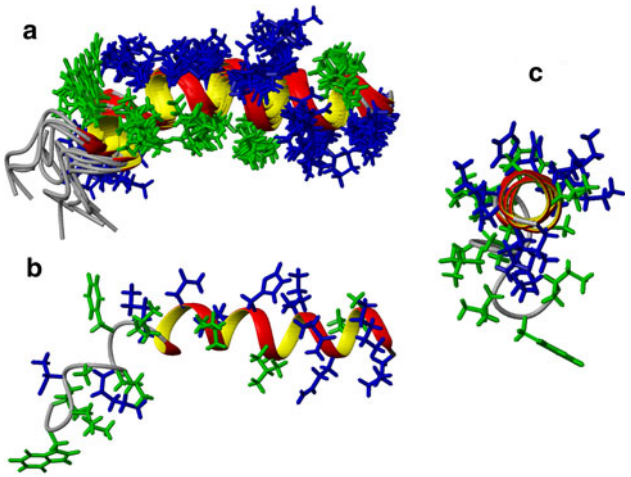


**Fig. 8** NMR structures of LyeTx I in 400 mM $DPC_{d38}$ micelles in phosphate buffer, pH 7.0 Panel **a** shows the 20 lowest energy structures. The hydrophobic residues are represented in blue and the hydrophilic and charged residues in green. Panel **b** and **c** show the lowest energy structure obtained for LyeTx I in $DPC_{d38,}$ viewed from the side and along the helix axis, respectively

**Table 2** Summary of the data on NOE restraints and calculated structures of LyeTx I in DPC micelles

| NOE restraints | LyeTx I |
|---|---|
| Total number of distance restrains | 370 |
| Number of intraresidue restrains | 198 |
| Number of sequential restrains ($i$, $i + 1$) | 91 |
| Number of medium range restrains $(i, i + j)_{j=2,\ 3,\ 4}$ | 81 |
| RMSD (Å)—all residues[a] | |
| Backbone | 1.95 |
| Backbone and heavy atoms | 2.65 |
| RMSD (Å)—helical segment[a,b] | |
| Backbone | 0.80 |
| Backbone and heavy atoms | 1.38 |
| Ramachandran plot analysis[c] | |
| Residues in most favoured regions | 86.4% |
| Residues in additional allowed regions | 13.3% |
| Residues in generously allowed regions | 0.0% |
| Residues in disallowed regions | 0.0% |

[a] Data from MOLMOL using the 20 lowest energy structures; [b] from L-6 to L-25; [c] data from PROCHECK-NMR

C-terminal portion and this can have an impact on the detailed peptide mechanism of interaction with bilayers. Considering the preference of tryptophan residue for membrane interfaces (Ulmschneider and Sansom 2001), its location in the N-terminal portion of LyeTx I can be important to anchor the peptide in the phospholipid media (Fig. 8b, c).

The statistics of the structural analysis of LyeTx I in the presence of DPC micelles are summarised in Table 2. The RMSD values obtained for the whole chain suggested a considerable conformational flexibility. However, these values declined significantly when only the helical segment was considered. The majority of the torsional angles were found in the most favoured or in the additionally allowed regions of the Ramachandran plot, indicating a good quality of the structures. The few residues observed in the disallowed regions are from residues close to the N-terminus, i.e. the non-structured part of the peptide (Table 2).

## Conclusion

The secondary structure and the antimicrobial activity of a new molecule, LyeTx I (2831.10 Da) from the venom of the spider *L. erythrognatha* are reported. LyeTx I showed a potent antimicrobial activity against all microorganisms tested, proving to be more active towards gram-positive bacteria (*S. aureus*) when compared to Gram-negative (*E. coli*) bacteria or yeasts (*Candida krusei* and *Cryptococcus neoformans*). A weak haemolytic activity was observed in higher concentrations of the peptide. The propensity of LyeTx I to form α-helix, as verified by CD and NMR spectroscopies, were compatible with the required conditions to initiate its antimicrobial action.

The affinity of LyeTx I for membrane bilayers (POPC) was unaffected by the presence of ergosterol, which is a lipid characteristic of fungi membranes. Nevertheless, the presence of cholesterol decreased the affinity of LyeTx I for membranes. Such apparent lipid specificity and the absence of toxicity in mice (data not shown) added to the possibility of obtaining this molecule by chemical synthesis, could indicate LyeTx I as a valuable tool for a rational design for developing antibiotics. However, the haemolytic activity, observed in vitro, could limit the therapeutic use of this molecule. A similar example was reported for Lycotoxin I and Lycotoxin II from the spider *L. carolinensis* (Adao et al. 2008). In this case, shortened analogues seem to have a decreased haemolytic activity. Therefore, what is proposed here is that the chemical manipulation of such molecules could generate some optimised derivatives with adequate characteristics to turn them into a possible therapeutic drug.

**Acknowledgements** This work was supported by FAPEMIG, MCT-FINEP, CAPES, CNPq and INCTTOX-Fapesp. Authors would like to thank Dr C. Bloch Jr for his stimulating discussions de novo sequencing in mass spectrometry.

## References

Adao R, Seixas R, Gomes P, Pessoa JC, Bastos M (2008) Membrane structure and interactions of a short Lycotoxin I analogue. J Pept Sci 14:528–534

Bechinger B (2004) Membrane-lytic peptides. Crit Rev Plant Sci 23:271–292

Boman HG, Hultmark D (1987) Cell-free immunity in insects. Annu Rev Microbiol 41:103–126

Budnik BA, Olsen JV, Egorov TA, Anisimova VE, Galkina TG, Musolyamov AK, Grishin EV, Zubarev RA (2004) De novo sequencing of antimicrobial peptides isolated from the venom glands of the wolf spider *Lycosa singoriensis*. J Mass Spectrom 39:193–201

Chan WC, White PD (2000) Fmoc solid phase peptide synthesis: a practical approach. Oxford University Press, Oxford

Chen Y, Mant CT, Farmer SW, Hancock RE, Vasil ML, Hodges RS (2005) Rational design of α-helical antimicrobial peptides with enhanced activities and specificity/therapeutic index. J Biol Chem 280:12316–12329

Clinical and Laboratory Standards Institute (2002) Reference method for broth dilution antifungal susceptibility testing of yeasts; Approved Standard (M27-A2), 2nd edn. Clinical and Laboratory Standards Institute, Wayne

Clinical and Laboratory Standards Institute (2007) Performance standards for antimicrobial susceptibility testing; seventeenth informational supplement. CLSI document M100-S17. Clinical and Laboratory Standards Institute, Wayne

Frezard F, Santaella C, Vierling P, Riess JG (1994) Permeability and stability in buffer and in human serum of fluorinated phospholipid-based liposomes. Biochim Biophys Acta 1192:61–70

Giacometti A, Cirioni O, Barchiesi F, Del Prete MS, Scalise G (1999) Antimicrobial activity of polycationic peptides. Peptides 20:1265–1273

Hemmi H, Ishibashi J, Hara S, Yamakawa M (2002) Solution structure of moricin, an antibacterial peptide, isolated from the silkworm *Bombyx mori*. FEBS Lett 518:33–38

Hernández-Ledesma B, Recio I, Amigo R (2008) β-Lactoglobulin as source of bioactive peptides. Amino Acids 35:257–265

Hyberts SG, Goldberg MS, Havel TF, Wagner G (1992) The solution structure of eglin C based on measurements of many NOEs and coupling constants and its comparison with X-Ray structures. Protein Sci 1:136–151

Kastin AJ (2006) Handbook of biologically active peptides. Academic, Amsterdam

Kuhn-Nentwig L (2009) Cytolytic and antimicrobial peptides in the venom of scorpions and spiders. In: De Lima ME, Pimenta AMC, Martin-Eauclaire MF, Zingali R, Rochat H(eds) Animal toxins: state of the art. Perspectives in health and biotechnology, 1st edn edn. Editora UFMG, Belo Horizonte, pp 153–172

Laskowski RA, Rullmann JA, MacArthur MW, Kaptein R, Thornton JM (1996) AUA and PROCHECK-NMR: programs for checking the quality of protein structures solved by NMR. J Biomol NMR 8:477–486

Liu ZH, Qian W, Li J, Zhang Y, Liang S (2009) Biochemical and pharmacological study of venom of the wolf spider *Lycosa singoriensis*. J Venom Anim Toxins incl Trop Dis 15:79–92

Martins RM, Sforca ML, Amino R, Juliano MA, Oyama S Jr, Juliano L, Pertinhez TA, Spisni A, Schenkman S (2006) Lytic activity and structural differences of amphipathic peptides derived from trialysin. Biochemistry 45:1765–1774

Matsuzaki K, Sugishita K, Fujii N, Miyajima K (1995) Molecular basis for membrane selectivity of an antimicrobial peptide, magainin 2. Biochemistry 34:3423–3429

Mor A, Nicolas P (1994) Isolation and structure of novel defensive peptides from frog skin. Eur J Biochem 219:145–154

Park JM, Jung JE, Lee BJ (1994) Antimicrobial peptides from the skin of a Korean frog, *Rana rugosa*. Biochem Biophys Res Commun 205:948–954

Pimenta AM, Rates B, Bloch C Jr, Gomes PC, Santoro MM, de Lima ME, Richardson M, Cordeiro Mdo N (2005) Electrospray ionization quadrupole time-of-flight and matrix-assisted laser desorption/ionization tandem time-of-flight mass spectrometric analyses to solve micro-heterogeneity in post-translationally modified peptides from *Phoneutria nigriventer* (Aranea, Ctenidae) venom. Rapid Commun Mass Spectrom 19:31–37

Prates MV, Sforca ML, Regis WC, Leite JR, Silva LP, Pertinhez TA, Araujo AL, Azevedo RB, Spisni A, Bloch C Jr (2004) The NMR-derived solution structure of a new cationic antimicrobial peptide from the skin secretion of the anuran *Hyla punctata*. J Biol Chem 279:13018–13026

Sanderson JM (2005) Peptide–lipid interactions: insights and perspectives. Org Biomol Chem 3:201–212

Sforça ML, Oyama S Jr, Canduri F, Lorenzi CCB, Pertinhez TA, Konno K, Palma Souza BM, MS Ruggiero, Neto J, Azevedo WF Jr, Spisni A (2004) How C-terminal carboxyamidation alters the biological activity of peptides from the venom of the eumenine solitary wasp. Biochemistry 43:5608–5617

Syvitski RT, Burton I, Mattatall NR, Douglas SE, Jakeman DL (2005) Structural characterization of the antimicrobial peptide pleurocidin from winter flounder. Biochemistry 44:7282–7293

Takeuchi K, Takahashi H, Sugai, M, Iwai H, Kohno T, Sekimizu K, Natori S, Shimada I (2004) Channel-forming membrane permeabilization by an antibacterial protein, sapecin: determination of membrane-buried and oligomerization surfaces by NMR. J Biol Chem 279:4981–4987

Ulmschneider MB, Sansom MS (2001) Amino acid distributions in integral membrane protein structures. Biochim Biophys Acta 1512:1–14

Verly RM, de Moraes CM, Resende JM, Aisenbrey C, Bemquerer MP, Piló-Veloso D, Valente AP, Almeida FC, Bechinger B (2009) Structure and membrane interactions of the antibiotic peptide dermadistinctin K by multidimensional solution and oriented 15N and 31P solid-state NMR spectroscopy. Biophys J 96:2194–2203

Xu K, Ji Y, Qu X (1989) Purification and characterization of an antibacterial peptide from venom of *Lycosa singoriensis*. Acta Zool Sin 35:300–305

Yan L, Adams ME (1998) Lycotoxins, antimicrobial peptides from venom of the wolf spider *Lycosa carolinensis*. J Biol Chem 273:2059–2066

Zasloff M (1987) Magainins, a class of antimicrobial peptides from *Xenopus* skin: isolation, characterization of two active forms, and partial cDNA sequence of a precursor. Proc Natl Acad Sci USA 84:5449–5453

Zasloff M (2002) Antimicrobial peptides of multicellular organisms. Nature 415:389–395